# AC Susceptibility and Electrical Properties of Tungsten Substituted $(Tl_{1-x}W_x)(BaSr)CaCu_2O_7$ superconductor

K. Muhammad-Najib and R. Abd-Shukor*

*Department of Applied Physics, Universiti Kebangsaan Malaysia*
*43600 Bangi, Selangor, Malaysia*
**Corresponding author email: ras@ukm.edu.my*

(Received: 10.7.2021 ; Published: 26.8.2021)

**Abstract.** This article reports on the effects of tungsten, W substitution at the Tl site of $(Tl_{1-x}W_x)(BaSr)Ca_2CuO_7$ superconductor. The samples were prepared through the solid-state reaction method. The resistance versus temperature curves were determined by using the four-point probe method. The AC susceptibility was measured and intergrain current density at the peak temperature of the imaginary part of the susceptibility χ", $J_c(T_p)$ was determined. The sample without W substitution showed the highest onset transition temperature, $T_{c\text{-onset}}$ at 108 K and zero-resistance temperature, $T_{c\text{-zero}}$ at 86 K. The susceptibility transition temperature, $T_{c\chi}$, decreased with W substitution. The peak temperature, $T_p$ of imaginary part of the susceptibility shifted to lower temperatures and broadened as W content was increased. This indicated that W weakened the flux pinning and intergrain coupling. $J_c(T_p)$ for $x$ = 0-0.4 were between 17 and 20 A cm$^{-2}$.

**Keywords:** Critical temperature; critical current density; flux pinning; x-ray diffraction

## I. INTRODUCTION

Elemental substitutions at various sites of cuprates based superconductor have been shown to enhance the superconducting properties of these materials. The Tl-based superconductor is one of the promising systems for nanoscale application [1, 2]. Due to its toxicity, the application of Tl based cuprates is somewhat limited. Substitution of various elements and compound at the thallium site improved the superconductivity of this system [3, 4]. However, other elemental substitutions suppressed the superconducting properties of the Tl system [5, 6].

The $TlSr_2CaCu_2O_7$ phase also known as Tl-1212 is interesting to study because it is not easy to prepare in the superconducting phase. This is due to the high formal average Cu valence state of +2.5, which is over-doped hole state [7]. Partial substitution with elements of higher valence state at different sites of Tl-1212 helps to decrease the average Cu valence state to the optimal value which is between +2.2 and +2.3 [8, 9]. Substitution of transition elements at various site of Tl-1212 enhanced the formation of superconducting phase [10, 11]. In addition, the presence of Ba and Sr with 1:1 ratio helps the formation of Tl-1212 phase [12, 13]. The highest $T_{c\text{-onset}}$ recorded for $(Tl_{0.6}Pb_{0.4})(BaSr)CaCu_2O_7$ is 108 K [13].

It is well-known that Cr substitution improved the Tl-1212 superconducting properties [14, 15]. Tungsten, W which belongs to the same group as Cr has not been widely studied. There are not many report on effect of W substitution on the thallium system. In $YBa_2Cu_3O_7$ superconductor, W nanoparticle does not affect the critical temperature of the system. However, the current density and flux pinning strength improved with W substitution [16]. The addition of W to the Bi-based system, $Bi_{1.6}Pb_{0.4}Sr_2Ca_2Cu_3O_{10}$ (Bi-2223) system lowers the transition temperature and phase formation [17].

It is interesting to study the effect of W on the superconducting properties of the Tl(BaSr)$CaCu_2O_7$. The objective of this study was to determine whether the Tl(BaSr)$CaCu_2O_7$ system can be further improved by W which has a smaller ionic radius compared to Tl as an alternative to Cr. Results from X-ray diffraction, DC electrical resistance measurement and AC susceptibility measurements are reported in this paper.

## II. EXPERIMENTAL DETAILS

The samples were prepared by the solid-state reaction method with nominal composition $Tl_{1-x}W_x(BaSr)CaCu_2O_7$ for $x$ = 0, 0.1, 0.2, 0.3 and 0.4. The precursor powder was prepared by mixing highly purity ($\geq$ 99.99%) $BaCO_3$, SrO and $CaCO_3$ with starting formula $(BaSr)CaCu_2O_y$. The mixture was ground in an agate mortar and heated at 900 °C for 24 h. Several intermittent grindings and heating were done to optimize the homogeneity of the precursor. $Tl_2O_3$ and $WO_3$ were then mixed with the precursor and presses into pellets with 13 mm diameter and 2 mm thickness. Excess 10 % $Tl_2O_3$ was added to compensate the thallium lost during the heating process. The pellets were placed in a preheated tube furnace at 980 $^oC$ with oxygen flow for 4 min.

The structure and phase of the samples were analyzed by X-ray powder diffraction (XRD) method using Bruker D8 Advance Diffractometer with $CuK_\alpha$ with angle $2\theta$ = 2° to 60°. From the XRD peaks in the pattern, the lattice parameters of Tl-1212 were calculated. The volume fraction of the phases were calculated based on Karaca et al. [18].

The electrical resistance-temperature measurements were carried out using the four-point probe method in conjunction with CTI Cryogenics Close Cycle Refrigerator Model 22 and Lakeshore Temperature Controller Model 235. The silver paint was used as electrical contacts. A Keithley 220 Programmable Current Source was used to supply a constant current ranging 1 mA to 100 mA. The room temperature electrical resistivity was measured by van der Pauw measurement method.

The AC susceptibility of bar shaped samples was measured using a susceptometer from Cryo Industry with model number REF -1808-ACS. An AC signal frequency of 295 Hz and 5 Oe magnetic field was used. The Bean model was used to determine the critical current density at the peak temperature, $T_p$ of $\chi$", $J_c(T_p)$ with formula $J_c(T_p) = H/(lw)^{1/2}$ where $H$ is applied field, $l$ and $w$ are the sample cross section dimensions [19].

## III. RESULTS AND DISCUSSION

The X-ray diffraction patterns in Figure 1 shows a single Tl-1212 phase for the non-substituted sample with tetragonal structure (space group P4/mmm). Other phases and impurities were observed in the XRD patterns of the W substituted samples namely Tl-1201, $Ca_{0.3}Sr_{0.7}CuO_2$ (CSCO) and $WO_3$ are indicated with *, # and $, respectively. In addition an unknown peak (β) was observed for both $x$ = 0.3 and 0.4 at $2\theta$ = 31.32 °. W substitution suppressed the Tl-1212 phase and other impurities were observed. The lattice parameter $a$, $c$ and the unit cell volume, $V$ are shown in Table 1. $V$ decreased with increase of W substitution because W ions has smaller ionic radii ($W^{+4}$ (0.66 Å), $W^{+5}$ (0.62 Å), and $W^{+6}$ (0.60 Å)) than $Tl^{+3}$(0.89 Å), it is likely that W ions have been substituted at the $Tl^{+3}$ site. W may have also resided at the interstitial sites. However, a more direct method is necessary to support these assertions. The volume fraction of phases present (as shown in Table 1) was determined using the following equations:

$$\Sigma I_{1212}(\%) = \frac{\Sigma I_{1212}}{\Sigma I_{1212} + \Sigma I_{1201} + \Sigma I_{CSCO} + \Sigma I_{WO3} + \Sigma I_{\beta}} \times 100$$

$$\Sigma I_{1201}(\%) = \frac{\Sigma I_{1201}}{\Sigma I_{1212} + \Sigma I_{1201} + \Sigma I_{CSCO} + \Sigma I_{WO3} + \Sigma I_{\beta}} \times 100$$

$$\Sigma I_{CSCO}(\%) = \frac{\Sigma I_{CSCO}}{\Sigma I_{1212} + \Sigma I_{1201} + \Sigma I_{CSCO} + \Sigma I_{WO3} + \Sigma I_{\beta}} \times 100$$

$$\Sigma I_{WO3}(\%) = \frac{\Sigma I_{WO3}}{\Sigma I_{1212} + \Sigma I_{1201} + \Sigma I_{CSCO} + \Sigma I_{WO3} + \Sigma I_{\beta}} \times 100$$

$$\Sigma I_{\beta}(\%) = \frac{\Sigma I_{\beta}}{\Sigma I_{1212} + \Sigma I_{1201} + \Sigma I_{CSCO} + \Sigma I_{WO3} + \Sigma I_{\beta}} \times 100$$

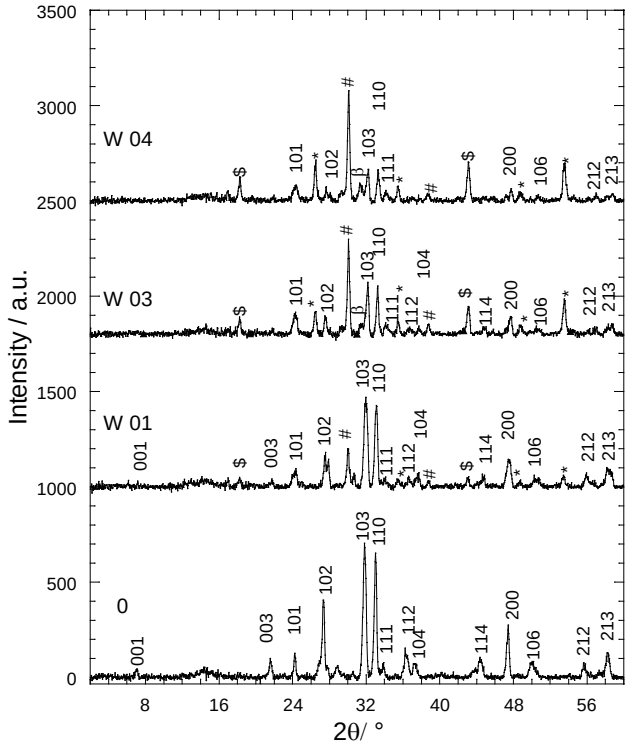


**Figure 1.** XRD patterns of $Tl_{1-x}W_x(BaSr)CaCu_2O_7$ for $x$ = 0, 0.1, 0.3, and 0.4. Peaks with (*), (#) and ($) indicate the Tl-1201, $Ca_{0.3}Sr_{0.7}CuO_2$ (CSCO) and $WO_3$, respectively. β denotes unknown impurity peak.

**Table 1.** Lattice parameters, unit cell volume and volume fraction for $Tl_{1-x}W_x(BaSr)CaCu_2O_7$. CSCO denotes $Ca_{0.3}Sr_{0.7}CuO_2$ and $V_\beta$ is an unknown impurity phase.

| $x$ | $a$ /Å | $c$ /Å | $V$ / Å$^3$ | $V_{\text{Tl-1212}}$ / % | $V_{\text{Tl-1201}}$/ % | $V_{\text{CSCO}}$ / % | $V_{\text{WO3}}$ / % | $V_\beta$ / % |
|---|---|---|---|---|---|---|---|---|
| 0 | 3.831 | 12.409 | 182.1 | >97 | - | - | - | - |
| 0.1 | 3.822 | 12.334 | 180.2 | 80 | 6 | 10 | 4 | - |
| 0.3 | 3.818 | 12.245 | 178.5 | 45 | 17 | 23 | 9 | 6 |
| 0.4 | 3.805 | 12.184 | 178.4 | 31 | 24 | 27 | 14 | 4 |

For a multilayered tetragonal cuprates, the lattice parameter *a* is mainly linked to the substitution and the carrier concentration while lattice parameter *c* is mainly linked to the

elemental arrangement, vacancies or substitution [20]. The contraction in lattice parameter *a* can be explained in terms of increase in the average copper valence state from lower W valence state for $Tl^{+3}$ which led to the compression of Cu-O bonding lengths within the copper oxygen sheets [21, 22]. The decrease in the *c* lattice parameter was probably due to ionic size effect as larger Tl ions were substituted by the much smaller W ions [22].

The temperature dependant DC electrical resistance curves showed metallic behaviour above $T_{\text{c-onset}}$ for all samples (Figure 2). The superconducting transition temperatures were between 80 K and 108 K. The non-substituted sample showed the highest $T_{\text{c-onset}}$ (108 K) and $T_{\text{c-zero}}$ (91 K) (Table 2). $T_{\text{c-onset}}$ decreased almost monotonically with increase in W substitution. $T_{\text{c-onset}}$ is associated with the variation of electronic structure in the normal state and the oxygen content which controls the charges transfer from chains to planes [16, 23]. As for $T_{\text{c-zero}}$, the monotonic decrease with increasing W substitution can be explained as due to the presence of non-superconducting phases which arises from the suppression by W. Weak coupling between impurities and superconductor grains, structural distortion as observed from the lattice parameters may explain the decrease of both $T_{\text{c-zero}}$ and $T_{\text{c-onset}}$. The room temperature resistivity, $\rho_{297\text{ K}}$ increased exponentially with W substitution indicating the scattering by impurities with W substitution.

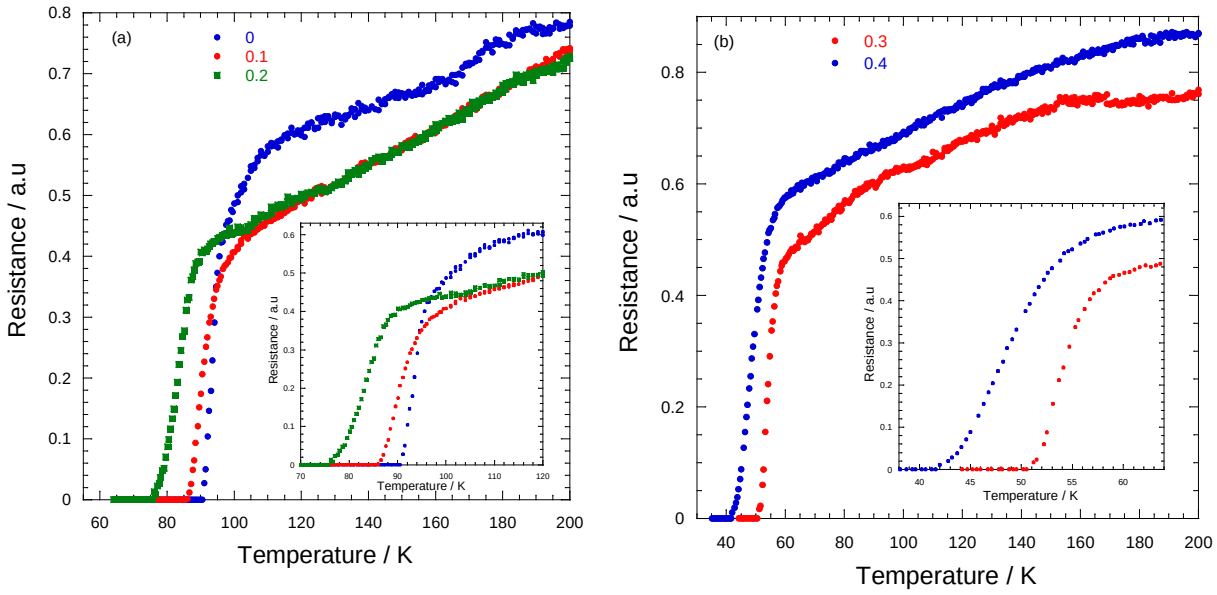


**Figure 2.** Electrical resistance versus temperature of $Tl_{1-x}W_x(BaSr)CaCu_2O_7$ for (a) $x$=0, 0.1, 0.2 and (b) $x$ = 0.3, and 0.4

**Table 2.** $T_{\text{c-onset}}$, $T_{\text{c-zero}}$, $\Delta T_c$, $T_{c\chi'}$, $T_p$, $J_c$ ($T_p$) and $\rho_{297K}$ for $Tl_{1-x}W_x(BaSr)CaCu_2O_7$

| $x$ | $T_{\text{c-onset}}$ / K | $T_{\text{c-zero}}$ / K | $\Delta T_c$ / K | $T_{c\chi'}$ /K | $T_p$ /K | $J_c(T_p)$/A cm$^{-2}$ | $\rho_{297\text{ K}}$ / mΩ cm |
|---|---|---|---|---|---|---|---|
| 0 | 108 | 91 | 17 | 97 | 80 | 18 | 3.04 |
| 0.1 | 103 | 86 | 17 | 85 | 78 | 17 | 2.66 |
| 0.2 | 95 | 76 | 19 | 46 | 35 | 17 | 7.02 |
| 0.3 | 60 | 51 | 9 | 57 | 46 | 18 | 16.5 |
| 0.4 | 60 | 42 | 18 | 35 | <20 | 20 | 64.5 |

Complex AC susceptibility ($\chi = \chi' + i\chi''$) curve as a function of temperature for all samples are shown in Figure 3. The diamagnetic shielding was observed for temperature below the

transition temperature, $T_{c\chi'}$ in all samples and indicated by the sudden decrease in the real part of the susceptibility, $\chi$'. The highest $T_{c\chi'}$ recorded for the non-substituted samples was 97 K. Due to low applied field used in this work, there were no intrinsic peak which represent intrinsic losses observed in imaginary part, $\chi$" of all samples. The observed peak in the imaginary part of susceptibility represents AC losses. The temperature at the peak of $\chi$", $T_p$ decreased gradually with W substitution. The non-substituted sample showed the highest $T_p$ of 80 K (Figure 4) . There were no peaks observed for $x$ = 0.4 in the 20 K - 120 K range. The decrease in $T_p$ indicates the weakening of inter-grain coupling and diminishing of the flux pinning strength. Table 2 shows $T_{c\text{-onset}}$, $T_{c\text{-zero}}$, $\Delta T_c$, $T_{c\chi'}$, $T_p$, $J_c$ ($T_p$) and $\rho_{297K}$ for $Tl_{1-x}W_x(BaSr)CaCu_2O_7$. At $T_p$ the flux penetration into the grains reach a maximum. The intergranular critical current density at $T_p$, $J_c(T_p)$ can be calculated since the magnitude of applied field, $H_{ac}$ (5 Oe) is equal to the penetrated flux at $T_p$. From the Bean model, $J_c(T_p)$ was calculated to be between 17 A cm$^{-2}$ and 20 A cm$^{-2}$.

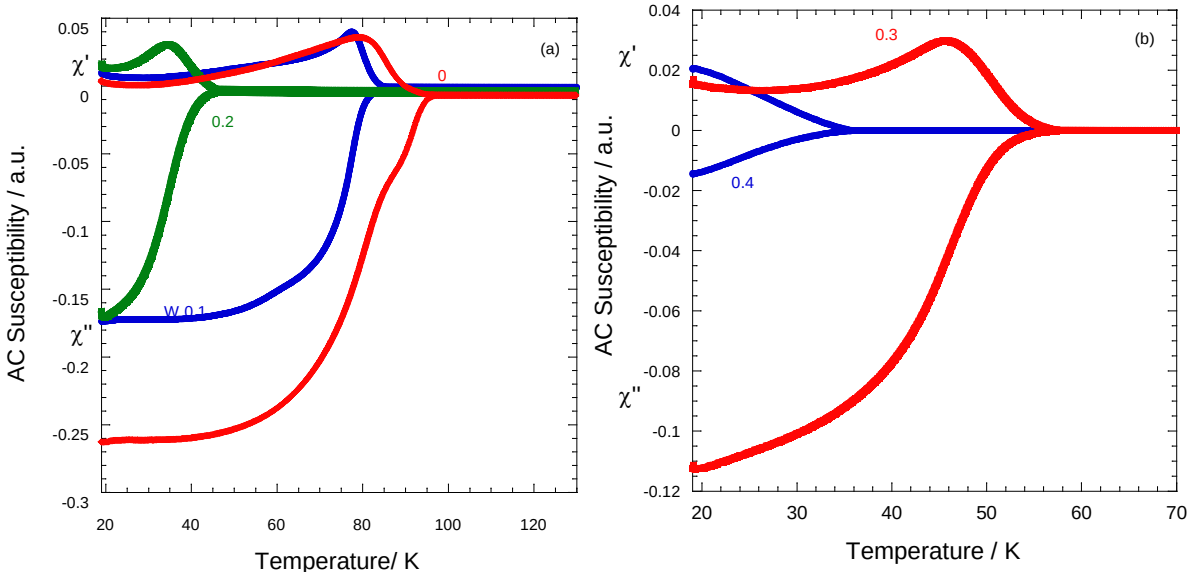


**Figure 3.** AC susceptibility ($\chi = \chi' + i\chi''$) versus temperature of $Tl_{1-x}W_x(BaSr)CaCu_2O_7$ for (a) $x$ = 0, 0.1, 0.2 and (b) $x$ = 0.3, and 0.4

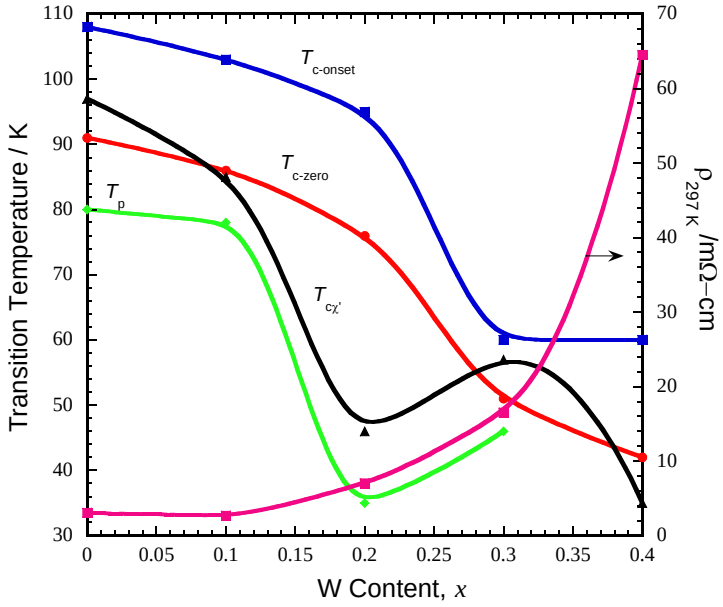


**Figure 4.** $T_{c\text{-onset}}$, $T_{c\text{-zero}}$, $T_{c\chi}$, $T_p$ and $\rho_{297\ K}$ versus W content of $Tl_{1-x}W_x(BaSr)CaCu_2O_7$ for $x$ = 0, 0.1, 0.2, 0.3 and 0.4

## VI. CONCLUSIONS

The effects of W substitution on $Tl_{1-x}W_x(BaSr)CaCu_2O_7$ for $x$ = 0, 0.1, 0.2, 0.3 and 0.4. were investigated. Partial substitution of W at the Tl-site suppressed the Tl-1212 superconducting phase. Our study showed that W may have entered the crystal lattice as the lattice parameters contracted due to the smaller W ionic radius relative to the Tl ions. The non-substituted sample showed the optimal superconducting properties with the highest $T_{c\text{-onset}}$, $T_{c\chi}$, and $T_p$. Substitutions of other multivalent elements with different ionic radius at the Tl-site of Tl-1212 are suggested for further studies.

## ACKNOWLEDGEMENTS

This research was supported by the Ministry of Higher Education of Malaysia under grant no. FRGS/1/2020/STG07/UKM/01/1.

## REFERENCES

1. Heiml, O. and Gritzner, G. (2002) *Superconductor Science and Technology* **15 (6)**, 956.
2. Sundaresan, A., Asada, H., Crisan, A., Nie, J., Kito, H., Iyo, A., Tanaka, Y., Kusunoki, M. and Ohshima, S. (2003) *Physica C* **388**, 473-474.
3. Jasim, K. A. (2008) *Journal for Pure and Applied Science* **21 (3)**, 806-813.
4. Jasim, K. A. (2013) *Journal of Superconductivity and Novel Magnetism* **26 (3)**, 549-552.
5. Abou Aly, A., Ibrahim, I., Awad, R., El-Harizy, A. and Khalaf, A. (2010) *Journal of Superconductivity and Novel Magnetism* **23 (7)**, 1325-1332.
6. Ahmad, N. H., Khan, N. A. and Yahya, A. K. (2010) *Journal of Alloys and Compounds* **492 (1)**, 473-481.
7. Subramanian, M. A., Torardi, C. C., Gopalakrishnan, J., Gai, P. L., Calabrese, J. C., Askew, T. R., Flippen, R. B. and Sleight, A. W. (1988) *Science* **242 (4876)**, 249.
8. Sheng, Z. Z., Li, Y. F. and Pederson, D. O. (1991) *Solid State Communications* **80 (11)**, 913-915.

9. Sheng, Z. Z., Xin, Y., Gu, D. X., Meason, J. M., Bennett, J., Ford, D. and Pederson, D. O. (1991) *Zeitschrift für Physik B Condensed Matter* **84 (3)**, 349-352.
10. Al-Sharabi, A. and Abd-Shukor, R. (2015) *Int. J. Electrochem. Sci* **10**, 140-150.
11. Abd-Shukor, R. and Lee, K. H. (1998) *Journal of Materials Science: Materials in Electronics* **9 (2)**, 99-102.
12. Mortada-Hamid, H., Ilhamsyah, A. B. P. and Abd-Shukor, R. (2020) *Journal of Materials Science: Materials in Electronics* **31 (7)**, 5316-5323.
13. Ranjbar, M., Ghoranneviss, M. and Abd-Shukor, R. (2018) *Applied Physics A* **124 (6)**, 1-6.
14. Ranjbar, G. and Abd-Shulor, R. (2012) *Physics International* **3 (2)**, 74-78.
15. Hamadneh, I., Kuan, Y. W., Hui, L. T. and Abd-Shukor, R. (2006) *Materials Letters* **60 (6)**, 734-736.
16. Slimani, Y., Almessiere, M. A., Hannachi, E., Baykal, A., Manikandan, A., Mumtaz, M. and Ben Azzouz, F. (2019) *Ceramics International* **45 (2, Part A)**, 2621-2628.
17. Türk, N., Gündoğmuş, H., Akyol, M., Yakıncı, Z. D., Ekicibil, A. and Özçelik, B. (2014) *Journal of Superconductivity and Novel Magnetism* **27 (3)**, 711-716.
18. Karaca, I., Uzun, O., Kölemen, U. Yilmaz, F. and Sahin, O. (2009). *Journal of Alloys and Compounds* **476**, 486–491.
19. Nikolo, M. (1995) *American Journal of Physics* **63 (1)**, 57-65.
20. Morosin, B., Venturini, E. L. and Ginley, D. S. (1991) *Physica C* **183 (1)**, 90-98.
21. Bakar, I. P. A. and Abd-Shukor, R. (2019) *Journal of Alloys and Compounds* **772**, 745-750.
22. Hamid, N. A., Musa, B., Yahya, A. K., Jumali, M. H. and Abd-Shukor, R. (2004) *Ceramics International* **30 (7)**, 1585-1589.
23. Zubair-Asyraf, J. M., Ilhamsyah, A. B. P. and Abd-Shukor, R. (2020) *Cryogenics* **105**, 103011.